Article has been reported and discussed at 17th International Conference on Advanced Laser Technologies, ALT09, 26 September – 01 October 2009, Antalya/Turkey.

THE EROSIVE LASER PLUME IONS COMPONENT RESEARCHES AT THE SILICON ABLATION IN VACUUM

E.V.KHAYDUKOV, V.V.ROCHEVA, A.A. LOTIN, O.A.NOVODVORSKY, V.Ya.PANCHENKO

Institute on Laser and Information Technologies of the Russian Academy of Sciences (ILIT RAS), 1 Svyatoozerskaya St.,140700 Shatura, Moscow Region, Russia

For the first time it is informed on engineering of the modified crossed-beam pulsed laser deposition method (CBPLD) which allows operating deposited particles energy in a wide range. By the Langmuir probe technique silicon ions time-of-flight curves (TFC) for the plasma beam formed by the crossed plumes from two silicon targets and the erosion plume from one silicon target are received. It is shown that ions TFC of the erosion plume approximate by the sum of one-dimensional Maxwell velocity distributions. Ions concentration change in initial plumes as a result of interaction is measured. Energy spectrum change of the plasma beam formed by the crossed plumes by means of angle change between them is shown.

1. INTRODUCTION

Silicon is widely applied in electronics and optoelectronics devices. Engineering of cheap technology of the ultrathin silicon films deposition would allow to introduce multilayer (which includes silicon layers) structures creation process (materials for spintronics, solar cells) in already existing silicon technologies [1,2]. One of the advantageous processes of the epitaxial thin films production is the pulsed laser deposition method (PLD) [2,3].

It is necessary to avoid drops falling on the substrate at the thin silicon films creation by the PLD method [2,4-6].

Efficient method of drops separation in the PLD method is the crossed plumes scheme of two erosive plumes [7,8]. Plume particles energy is rendered significant influence on properties of the received film (type of crystal structure, crystals size, adhesion, epitaxy, etc.) besides drops [9]. Therefore the important characteristics of the pulsed laser deposition process are a plume energy spectrum monitoring and control in particular an ions energy spectrum [3,9-11] directly during the thin film growth. It is especially important to control the energy spectrum at the multilayer ultrathin films deposition [12].

In the present work by the Langmuir probe technique ions velocity distributions of the plume at one silicon target ablation and of the plasma beam formed by the crossed plumes at two silicon targets ablation by radiation of the first harmonic of the solid-state laser (λ =1,06 μm) are investigated. The ions time-of-flight curves (TFC) are received at the probe-to-target distances in the 25-120 mm range. TFC approximation by the sum of one-dimensional Maxwell velocity distributions for several ions groups is spent. For the first time ions energy spectrum control possibility at the crossed plumes method by means of angle changing between initial plumes axes is shown.

2. EXPERIMENTAL SETUP

The experimental setup scheme is presented on fig. 1. Experiments were performed in the vacuum chamber which was pumped by turbo-molecular pump to 10^{-6} Torr pressure. Disk form targets from monocrystalline silicon were fixed in the holder and rotated for homogeneous target yield. Laser erosion plasma from the silicon target was formed by the influence of the first harmonic Q-switching YAG:Nd^{3+} laser radiation. Pulse duration made 15 ns, pulse energy was 50 - 500 mJ. The beam divides into two equal parts which radiation was focused on the targets surface.

Langmuir probe of 5.5 mm length was fabricated from 0.16 mm diameter tungsten wire. The probe placed perpendicularly plume axes. Probe moving in the vacuum chamber was carried out along the erosion plume axis in 25-120 mm range. The probe potential could change in limits from 0 to -20 V. As a source of the probe variable voltage was the storage battery which through a potentiometer was connected by one pole to the probe and by other pole through the pull-up resistor was earthed. For the probe potential stabilization during current flow the source of variable voltage was bridged by 2.5 μF capacity. The probe current was registered on 1 k Ω pull-down resistor with use of a high-speed AT-5102 (International Instruments) analog-to-digital converter (ADC) and saved to the PC. Charges time of arrival to the probe reading was performed from the laser pulse generation moment registered by the photodiode the signal from which delivered on the ADC starting channel.

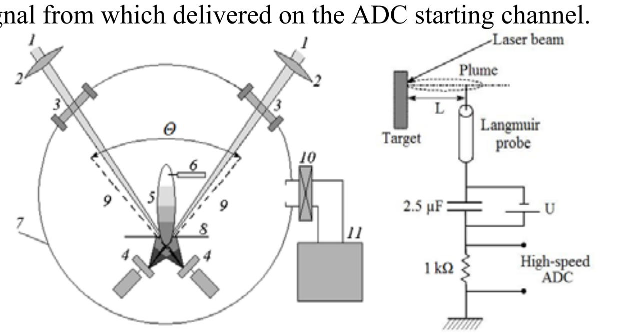

Fig.1. Experimental setup scheme and electrical schematic of the plasma beam probe researches at the silicon ablation: 1 – YAG:Nd^{3+} laser radiation, 2 – focusing lenses, 3 – window of the vacuum chamber, 4 - target, 5 – plasma beam, 6 – Langmuir probe, 7 – vacuum chamber, 8 - diaphragm, 9 – erosion plume axis, 10 - vacuum seal, 11 – turbo-molecular pump.

In the crossed plumes mode the angle between targets and accordingly between plumes axes changed from 180^0 to 70^0. Targets rotation axes placed in one plane. The fixed shield with an aperture mounted perpendicularly bisector of the angle formed by the plumes axes. The aperture diameter selected such to exclude direct visibility of the targets ablation areas from the probe location than the direct hit on the probe of the charged particles from initial plumes was excluded. At one of initial plumes research the signal of the probe located on the plume recession axis was registered, the second plume was blocked, the shield was not mounted.

3. RESULTS AND DISCUSSION

In the spent experiments the ions probe current TFC have been received in a case of the silicon ablation at various probe-to-target distances at different laser radiation energies. On fig. 2 are demonstrated the TFC at 32 J/cm^2 energy density on the target, time was counted from the ablation moment. At energy density decrease on the silicon targets the form of the TFC does not change.

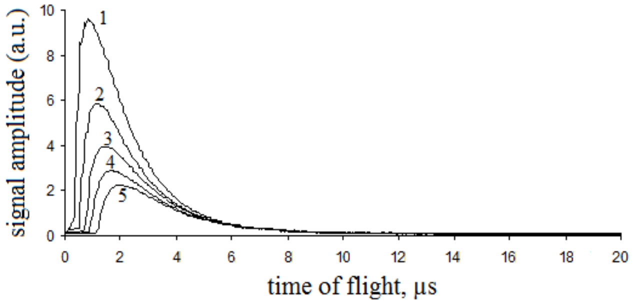

Fig. 2. Probe time-of-flight curves of the erosion plume from one target at various probe-to-target distances: 1 – 35 mm, 2 – 55 mm, 3 – 75 mm, 4 – 95 mm, 5 – 115 mm. Probe potential -18 V.

The ions TFC for have one strongly pronounced maximum with sharp rise-up portion and more flat descending part which is receding to zero approximately of 15 µs. All TFC have been received in the time range from 0 to 50 µs but on fig. 2 time interval is reduced to 20 µs for the best resolution. The TFC signal amplitude at probe-to-target distance increase decreases inversely to probe-to-target squared distance as a result of plume expansion.

From fig. 2 it is visible that the rise-up portion signal delay is proportional to probe-to-target distance. The ions leading group times of arrival from probe-to-target distance in 25-115 mm range have been determined. Time of arrival was determined by the delay between the targets ablation moment and the maximum of the probe signal. At three various energy densities on the target this dependence has linear character. The received dependences are demonstrated on fig. 3.

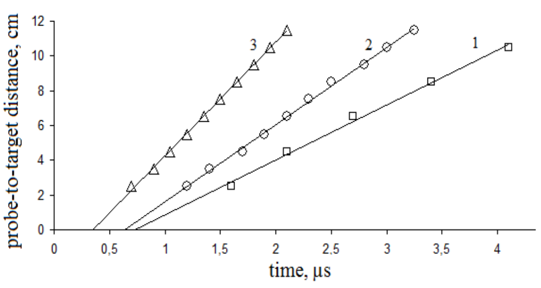

Fig.3. The time-of-flight curves peak time of arrival dependence on probe-to-target distance of the erosion plume from one target at the various energy density: 1 - 10 J/cm^2, 2 - 16 J/cm^2, 3 - 32 J/cm^2.

From fig. 3 it is visible that the silicon ions lead group recession velocity does not depend on distance to the target and at 32 J/cm^2, 16 J/cm^2, 10 J/cm^2 energy density makes 53 km/s, 31 km/s, 25 km/s accordingly.

Asymmetry of the probe curves presented on fig. 2 is connected with nonequilibrium ions velocity distribution in the plume [10]. All the received TFC are well approximated by the sum of several Maxwell curves with different positions of maxima:

$$I(t) = KLt^{-4} \exp\left[-\frac{2(L/t)^2}{\nu^2}\right], \qquad (1)$$

where K – proportionality coefficient; ν – the most probable velocity; L – probe-to-target distance, t – time. Approximation was spent from the assumption that at the plume there are singly charged ions with m weight and the charged particles with nm weights, where n = 2,3,4 …. So for the plume from one target at 32 J/cm^2 energy density for all the measured probe-to-target distances the TFC are approximated by the sum of six groups of positive charged particles spreading with the velocities: 57.7 km/s; 40.8 km/s; 33.3 km/s, 28.9 km/s, 25.8 km/s and 23.6 km/s.

On fig. 4 are presented the TFC for 65 and 105 mm probe-to-target distances and their approximation by the sum of six Maxwell curves. It is visible that the total curves are labeled on fig. 4 by circles coincide with the experimental TFC.

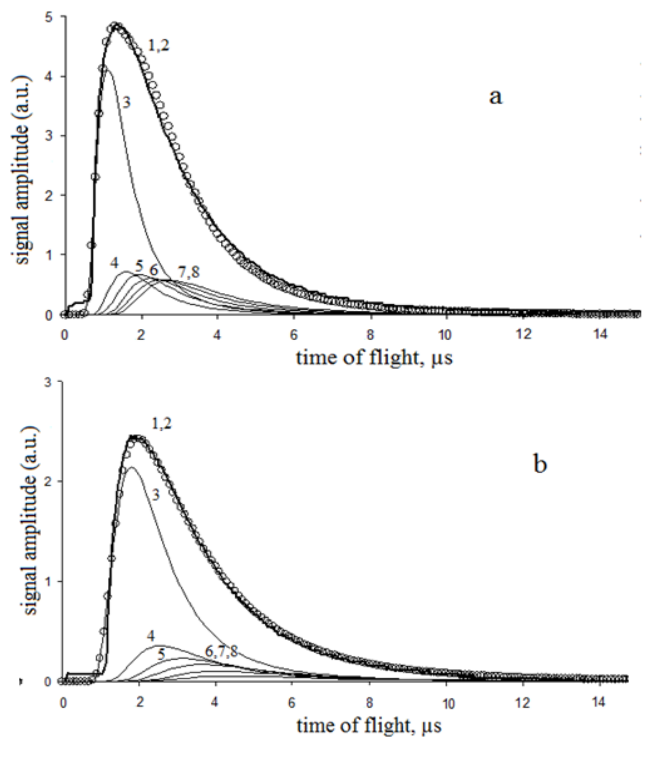

Fig.4. Experimental time-of-flight curves of the erosion plume from one target for 65 mm (a) and 105 mm (b) probe-to-target distances and their approximate by the sum of six Maxwell curves. By thick firm line is labeled experimental curve 1, by circles is labeled theoretical curve 2 that be the sum of Maxwell curves 4, 5, 6, 7 and 8 with 57.7 km/s, 40.8 km/s, 33.3 km/s, 28.9 km/s, 25.8 km/s and 23.6 km/s velocities.

The TFC of the deflected beam formed by the crossed plumes (fig. 1) at different angles and at various energy densities on the silicon targets have been received. The probe moved along the deflected beam axis, the distance was measured from diaphragm position. On fig. 5 are presented the experimental TFC of the deflected beam formed after the initial plumes crossing at 90 degrees angle at different probe positions relative to the diaphragm. The TFC amplitude decreased inversely to squared distance as well as for the case of the plume from one target.

The TFC maximum time of arrival as well as for the case of the plume from one target changes linearly at change of the probe position (insert on fig. 5) that indicate of inertial recession of the beam charged particles.

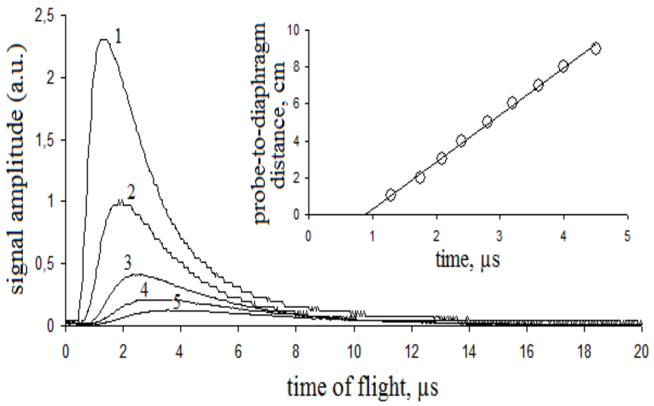

Fig.5. Probe time-of-flight curves of the plasma beam formed by the crossed plumes at various probe-to-diaphragm distances: 1 – 10 mm, 2 – 30 mm, 3 – 50 mm, 4 – 70 mm, 5 – 90 mm. Angle Θ between plumes axes made 90^0. Probe potential -18 V. Energy density - 32 J/cm^2. On insert: the time-of-flight curves peak time of arrival dependence on probe-to-diaphragm distance.

Comparing the ions TFC of the erosion plume from one target (fig. 2) and the beam spreading on the bisector between initial plumes axes (fig. 5) it is possible to see that not all ions which are present at initial plumes deflect at interaction. From TFC of the probe placed on one of the plumes recession diagram axis behind the plumes crossing area at 120 mm distance from the target (at the diaphragm 8 absence, fig. 1) ions concentration was determined at presence and absence of the second plume (insert on fig. 6). The Θ angle between plumes axes made 90^0. Such probe location excluded hit on it of the charged particles from the second plume. The results are presented on fig. 6 where the curve 1 shows concentration distribution in the plume from the A target at the B target ablation absence, the curve 2 shows concentration distribution in the plume from the A target at the A and B targets ablation. The difference between curves corresponds to the deflected part of the plume. It is visible that the considerable part of the plume deflects.

At the angle change between initial plumes axes the TFC maximum of the deflected beam moves, the probe position is fixed (6 on fig. 1). Fig. 7 demonstrates the shift of the deflected beam TFC maximum at the Θ angle change between initial plumes axes from 90^0 to 170^0. It is possible to calculate velocities of the deflected ions after interaction considering plumes recession velocity till the crossing moment and knowing a way passed by ions before and after crossing.

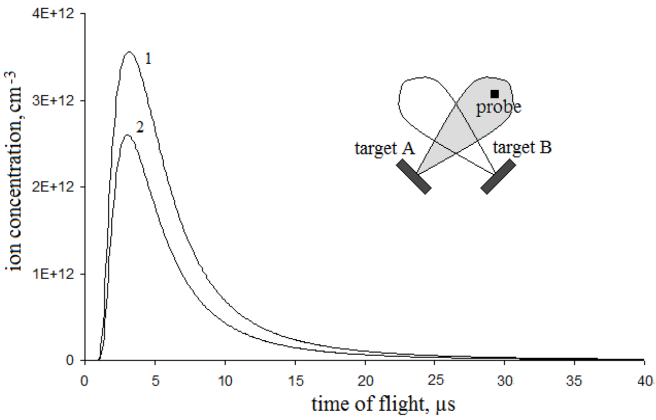

Fig.6. Ions concentration change in the plume at 120 mm probe-to-target distance. 1 – probe on plume axis at the A target ablation, 2 - probe on plume axis at the A and B targets ablation. Angle Θ between plumes axes made 90^0. On insert: scheme of the experiment.

At the angle change between initial plumes axes the TFC maximum of the deflected beam moves, the probe position is fixed (6 on fig. 1). Fig. 7 demonstrates the shift of the deflected beam TFC maximum at the Θ angle change between initial plumes axes from 90^0 to 170^0. It is possible to calculate velocities of the deflected ions after interaction considering plumes recession velocity till the crossing moment and knowing a way passed by ions before and after crossing.

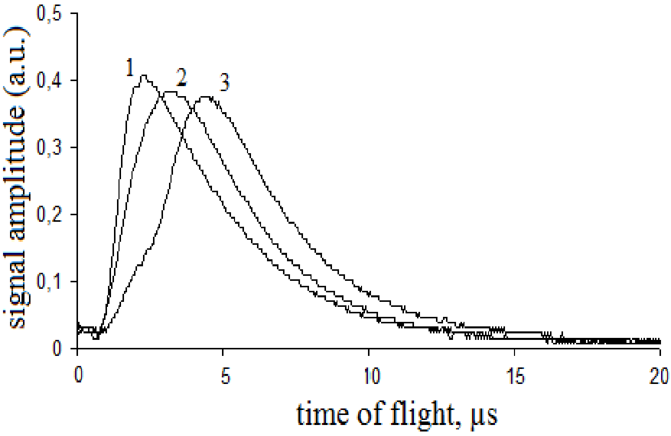

Fig.7. Probe time-of-flight curves at the angle change between initial plumes axes. 1 – 170^0, 2 – 130^0, 3 – 90^0 at 50 mm probe-to-diaphragm distance. Probe potential -18 V. Energy density - 32 J/cm^2.

It allows to determine kinetic energy change of the leading ions in the deflected beam at the angle change between initial plumes axes. Kinetic energy change of the leading ions from the angle between initial plumes axes is presented on fig. 8.

From fig. 8 it is visible that at angle change from 170 to 70 degrees between plumes axes the ions leading group energy changes from 92 to 480 eV at 32 J/cm^2 energy density on the target. For comparison on fig. 8 value of the ions leading group energy which is equal 677 eV is presented at one silicon target ablation (it is labeled by triangle on fig. 8) at other similar conditions.

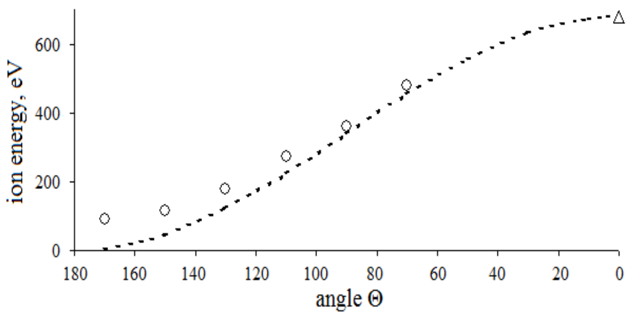

Fig.8. Ions leading group energy change for the plasma beam formed by the crossed plumes from the angle between initial plumes axes at 32 J/cm^2 energy density on the silicon target.

In the figure by the dotted line is presented a theoretical curve for the particles energy in the deflected beam with the assumption of conservation of the ions initial velocity tangential component at the collisional process. Character of the deflected ions energy change qualitatively is matching to the offered model. Quantitative mismatching of the experimental data is connected with presence of particles recession angle dispersion in the initial plumes. The additional energy increase of the deflected beam particles can be caused by heating of the initial plumes crossing area at inelastic collision.

4. CONCLUSIONS

By the Langmuir probe technique the erosion plume characteristics at silicon ablation by the Q-switching YAG:Nd^{3+} laser are investigated.

Silicon ions lead group recession velocity does not depend on distance to the target at one silicon target ablation and in plasma beam formed by the crossed plumes at two silicon targets ablation.

The TFC are received at the probe-to-target distances in the 25-120 mm range. TFC approximation by the sum of one-dimensional Maxwell velocity distributions for several ions groups is spent. For the first time it is informed on engineering of the modified crossed-beam pulsed laser deposition method which allows operating deposited particles energy in a wide range.

4. ACKNOWLEDGMENTS

Work is executed with support of RFBR grants 09-08-00291, 09-02-12108, 09-08-01053, 09-02-01298, 09-07-12151.

[1]. *M.Bolduc, C.Awo-Affoud, A.Stollenwerk, et al.,* Phys. Rev. B. 71, 033302-033305 (2005).

[2]. *S.Yasuda, T.Chikyow, S.Inoue, N.Matsuki, K.Miyazaki, S. Nishio, M.Kakihana, H.Koinuma,* Appl. Phys. A. 69, S925-S927 (1999).

[3]. *V.Ya.Panchenko, O.A.Novodvorsky, V.S.Golubev,* Science and technology in industry. 4(1), 39-51 (2006).

[4]. *E.V.Khaydukov, A.A.Lotin, D.N.Melnikov, O.A.Novodvorsky, V.Ya.Panchenko,* Proceedings of IX Interuniversity scientific school of young experts «The concentrated energy streams in the space technology, electronics, ecology and medicine», 127-131 (2008).

[5]. *A.Masuda, K.Matsuda, S.Usui, T.Minamikawa, T.Shimizu, A.Morimoto, Y.Yonezawa,* Mater. Sci. Eng. B. 41, 161-165 (1996).

[6]. *E.V.Khaydukov, A.A.Lotin, O.A.Novodvorsky, V.Ya.Panchenko, V.V.Rocheva,* The Collection of scientific and technical sections reports theses of the International Forum on Nanotechnology, Part 1, 771-772 (2008).

[7]. *M.D.Strikovsky, E.B.Klyuenkov, S.V.Gaponov, , J.Schubert, C.A.Copetti,* Appl. Phys. Lett. 63 (8), 1146-1148 (1993).

[8]. *A.Gorbunov, A.Tselev, W.Pompe,* , Proc. SPIE 3688, 351-358 (1999).

[9]. *K.L.Saenger,* J. Appl. Phys. 70, 5629-5635 (1991).

[10]. *R.Eason,* Pulsed laser deposition of thin films: Applications-LED growth of functional materials, N.J.:Wiley-Interscience, Hoboken, (2007).

[11]. *O.A.Novodvorsky, E.O.Filippova, O.D.Khramova, A.K.Shevelev, C.Wenzel, J.W.Bartha,* Quantum Electronics. 31(2), 159-163 (2001).

[12]. *H.Mai, R.Dietsch, T.Holz, S.Voellmar, S.Hopfe, R.Scholz, Peter Weissbrodt, R.Krawietz, B.Wehner, H.Eichler, H.Wendrock,* Proc. SPIE 2253, 268-279 (1994).